แบบรายงานการวิจัย

ทุนพัฒนาอาจารย์ใหม่/นักวิจัยใหม่

เรื่อง Value of Dynamic Contrast-Enhanced Magnetic Resonance Imaging for Determining the Plasma Epstein - Barr Virus Status and Staging of Nasopharyngeal Carcinoma

โดย

แพทย์หญิงณัชวาล จิตตภิรมย์ศักดิ์

รองศาสตราจารย์ นายแพทย์ชวลิต เลิศบุษยานุกูล (อาจารย์ที่ปรึกษา)

ภาควิชารังสีวิทยา คณะแพทยศาสตร์ จุฬาลงกรณ์มหาวิทยาลัย

Value of Dynamic Contrast-Enhanced Magnetic Resonance Imaging for Determining the Plasma Epstein - Barr Virus Status and Staging of Nasopharyngeal Carcinoma

Aniwat Sriyook[1], Chawalit Lertbutsayanukul[2], Nutchawan Jittapiromsak[1,*]

[1]Division of Diagnostic Radiology, Department of Radiology, Faculty of Medicine, Chulalongkorn University, King Chulalongkorn Memorial Hospital, The Thai Red Cross Society, Bangkok, Thailand

[2]Division of Radiation Oncology, Department of Radiology, Faculty of Medicine, Chulalongkorn University, King Chulalongkorn Memorial Hospital, The Thai Red Cross Society, Bangkok, Thailand

Running title: Utility of DCE MRI for patients with NPC

*Corresponding author: Nutchawan Jittapiromsak, Division of Diagnostic Radiology, Department of Radiology, Faculty of Medicine, Chulalongkorn University, King Chulalongkorn Memorial Hospital, The Thai Red Cross Society, 1873 Rama IV Rd., Pathumwan, Bangkok 10330, Thailand; Tel: +662-256-4417; Fax: +662-256-4417; E-mail: nutchawan.j@chula.ac.th

Abstract

Objective: To determine the associations between dynamic-contrast enhanced (DCE) magnetic resonance imaging (MRI) parameters and plasma Epstein-Barr virus (EBV) DNA status and nasopharyngeal carcinoma (NPC) stages.

Methods: We prospectively studied the DCE MRI results of 47 patients with newly diagnosed NPC and a known pre-treatment plasma EBV DNA level. Regions of interest (ROIs) were drawn at primary tumors, and DCE MRI parameters, including mean and max values of Ktrans, Kep, Ve, and Vp, were recorded. Spearman's rank correlation was used to identify significant associations between DCE MRI parameters and plasma EBV DNA level and NPC stages. Mann-Whitney U tests and unpaired *t*-test were performed to compare DCE MRI parameters among groups and to find optimal cut-off values using receiver operating characteristic curves.

Results: DCE MRI parameters were correlated with plasma EBV DNA levels and NPC stages. Positive plasma EBV DNA was correlated with lower Kep_{mean} (optimal cut-off value, 2.1 min^{-1}; area under the curve [AUC], 0.714) and higher Ve_{max} (optimal cut-off value, 0.675; AUC, 0.706). Ve_{max} higher than 0.765 (AUC, 0.678) was correlated with plasma EBV DNA ($\geq$ 2,300 copies ml^{-1}). Higher $Ktrans_{max}$ (cut-off value, 1.495 min^{-1}; AUC, 0.767) was correlated with high T stage, and higher Vp_{mean} (cut-off value, 0.125; AUC, 0.739) was correlated with positive lymph nodes. $Ktrans_{max}$ higher than 1.495 min^{-1} (AUC, 0.711) was correlated with the high stage group.

Conclusions: DCE MRI is correlated with the plasma EBV DNA status and NPC stages. Therefore, DCE MRI findings may be used as imaging biomarkers for NPC patients.

Keywords: DCE MRI, Plasma EBV DNA, staging, nasopharyngeal carcinoma

Introduction

Nasopharyngeal carcinoma (NPC) is the most common primary malignancy arising from the nasopharynx. Its incidence varies based on the geographic location, but is more pronounced in Asian countries, especially in Southern China and Southeast Asia, including Thailand, which is known to be an endemic area. Age-standardized incidences are up to 25.0 per 100,000 males and 9.0 per 100,000 females in Southern China, whereas they are up to 5.4 per 100,000 males and 1.6 per 100,000 females in Thailand.[1] According to the World Health Organization, NPC can be categorized into three types: 1) keratinizing squamous cell carcinoma, 2) nonkeratinizing carcinoma (differentiated and undifferentiated), and 3) basaloid squamous cell carcinoma.[2] Nonkeratinizing undifferentiated carcinoma is the most common type of NPC in endemic areas and has a very strong association with Epstein-Barr virus (EBV) infection.[3, 4]

EBV is a double-stranded DNA virus that can establish two modes of a life cycle in the host: lytic and latent. The underlying mechanism of NPC caused by EBV remains unclear; however, the latent mode of EBV infection is considered to play a major role in the pathogenesis of NPC.[5] EBV can be detected in various specimens, including plasma, peripheral blood cells, and biopsy tissue. Of these, plasma EBV DNA is more widely accepted in clinical settings of NPC because it serves as a reliable biomarker for detection, monitoring, and prognosis.[3-6] It has been reported that pre-treatment plasma EBV DNA ($\geq$ 2,300 copies ml^{-1}) could predict the overall survival, progression-free survival, and distant metastatic-free survival rates of patients with NPC.[7]

Dynamic contrast-enhanced (DCE) magnetic resonance imaging (MRI) is an MR perfusion technique that uses rapid sequential image acquisitions from an area of interest before, during, and after bolus administration of contrast media.[8] This technique can be used as a

noninvasive method for the evaluation of blood flow, blood volume, and wash-in/washout properties, as well as capillary endothelial permeability in the tumor.[8, 9] One of the hallmark features of cancer is angiogenesis, which provides blood flow and oxygen for the growth of cancer cells. However, these new abnormal vessels are tortuous and leaky, leading to increased vascular permeability, which can be detected by DCE MRI.

DCE MRI has a potential role in the evaluation of tumors, particularly in breast and prostate cancer. In head and neck tumors, DCE MRI can be used as an additional tool and may help clinicians to predict and evaluate treatment response, assess cervical nodal metastasis, differentiate post-treatment changes, and identify residual/recurrent tumors, as well as different types of head and neck cancers.[10-12] Only a few studies have determined the correlation between DCE MRI parameters with NPC stages, but no previous study has explored the existence of any association between DCE MRI parameters and the plasma EBV DNA status. Therefore, the primary objective of this study was to identify any association between DCE MRI parameters and plasma EBV DNA status, whereas the secondary objective was to verify the correlation between DCE MRI parameters and NPC stages, to determine whether DCE MRI may be used as an adjunct tool for patients with NPC to predict clinical outcomes.

Patients and methods

Subjects

This study was approved by the Institutional Review Board (IRB Number 689/60), and all study participants provided written informed consent. The inclusion criteria were as follows: 1) recent diagnosis (January 2018–2019) of NPC; 2) application of pre-treatment DCE MRI; and 3) evaluation of the pre-treatment plasma EBV DNA level. Exclusion criteria included: 1)

history of head or neck radiation or previous chemotherapy, and 2) degraded image quality or significant motion artifact(s). A total of 48 patients were recruited; one was excluded due to motion artifacts on the images. Data pertaining to sex, age, tumor pathology, American Joint Committee on Cancer (AJCC) Tumor, Node, and Metastasis (TNM) stages, stage groups, pre-treatment plasma EBV DNA levels, and values of DCE MRI parameters were recorded.

MR imaging protocol

Every patient underwent MRI simulation and pre-treatment DCE MRI within two weeks after evaluating the pre-treatment plasma EBV DNA level, using the same MRI scanner (1.5T GE Signa HDxt MRI; General Electric, Milwaukee, WI, USA) with a six Channel Flex phased-array coil and the same parameters. Standard imaging sequences included the axial fast spin-echo (FSE) T1-weighted image (TR 640 ms, TE 10 ms, NEX 1, FOV 24 × 24 cm, matrix size 256 × 384, slice thickness [ST]/slice spacing [SP] 3/3.3 mm], axial FSE T2-weighted image with fat suppression (TR 4860 ms, TE 81.37 ms, NEX 1, FOV 24 × 24 cm, matrix size 256 × 384, ST/SP 3/3.3 mm), DCE MRI, and post-gadolinium axial FSE T1-weighted image with fat suppression image (TR 640 ms, TE 10 ms, NEX 1, FOV 24 × 24 cm, matrix size 256 × 384, ST/SP 3/3.3 mm).

DCE MRI imaging was performed in 28 phases per examination using fast spoiled gradient recalled echo (FSPGR) (NEX 0.84, TR 8.42 ms, TE 3.49 ms, FOV 24 × 24 cm, matrix size 160 × 256, ST/SP 5/2.5 mm) with a total scan time of approximately 5 min. The first three phases were performed before Gadolinium administration. After the third phase, 0.2 ml kg^{-1} (0.1 mmol kg^{-1}) Gadoterate meglumine (DOTAREM®) was administered at a rate of 5 ml sec^{-1} and

flushed with 50 ml of normal saline. The post-gadolinium axial FSE T1-weighted image with fat suppression image was subsequently scanned after DCE MRI acquisition completion.

DCE MRI analyses

The DCE MRI data were post-processed using Olea Sphere 3.0 (Olea Medical, La Ciotat, France). Inversion time (TI) of tissue was 1,200 ms. Regions of interest (ROI) were drawn at the primary tumor independently by a neuroradiologist with nine years of experience and a second-year neuroradiology fellow; both were blinded to plasma EBV status and the NPC stages. The axial slice of the post-gadolinium 3D-FSPGR image that showed the maximum area of the tumor was selected (Fig 1A, 2A). We only used the axial image because it was more suitable in clinical practice than the whole tumor volume analysis. ROIs were drawn just inside the edge of the tumor, avoiding areas of necrosis and hemorrhage, to prevent subtle motion artifacts and air or normal soft tissue from the partial volume averaging effect. The neuroradiologist and neuroradiology fellow reached a consensus on the final selected ROIs. The mean and maximum values of DCE MRI parameters, including Ktrans, Kep, Ve, and Vp according to the extended Tofts model, were recorded.[13] Definitions of all parameters are provided in Table 1.

NPC staging and plasma EBV DNA detection

NPC was staged according to the eighth edition of the AJCC cancer staging criteria[2] following a consensus between a radiation oncologist and a radiologist. Patients were further divided into three major groups: 1) low- and high-T stages (T1–T2 and T3–T4, respectively); 2) N negative (N0) and N positive (N1–3); and 3) low- and high-stage groups (I–II and III–IV, respectively).

Blood samples were collected from every patient after the diagnosis of NPC and sent to a standard laboratory for the evaluation of the plasma EBV DNA level. EBV nucleic acids were purified from the plasma using the QIAsymphony SP and QIAsymphony DSP Virus/Pathogen Midi Kit (QIAGEN, Germany), according to the manufacturer's protocol. Eluates were transferred to 96-microwell plates for assembly using the artus EBV QS RGQ kit (QIAGEN), and aliquoted reactions were performed in a Rotor-Gene Q. PCR amplification conditions were as follows: 95°C for 10 min, followed by 45 cycles at 95°C for 15 sec, 65°C for 30 sec, and 72°C for 20 sec. The quantification of EBV DNA was carried out by using an RTQ-PCR system, targeting the BamHI-W fragment region of the EBV genome. A plasma EBV DNA concentration less than 316 copies ml^{-1} was defined as an undetectable level. Based on the concentration, plasma EBV DNA was categorized into two major groups: 1) negative or positive plasma EBV DNA (< 316 copies ml^{-1} and ≥ 316 copies ml^{-1}, respectively), and 2) plasma EBV DNA ($<$ and $\geq$ 2,300 copies ml^{-1}); the optimal cut-off value was as described previously.[7]

Statistical analysis

Spearman's rank correlation was applied to find any significant associations between DCE parameters and plasma EBV DNA levels, as well as AJCC T stages, N stages, and AJCC stage groups. The Shapiro-Wilk test was used to test if the DCE MRI data were normally distributed. The Mann-Whitney U test (for non-normally distributed data) and unpaired t-test (for normally distributed data) were performed to compare DCE MRI parameters between negative and positive plasma EBV DNA, plasma EBV DNA ($<$ and $\geq$ 2,300 copies ml^{-1}), low and high T stages, N negative and positive, as well as low and high stage groups. Significant DCE MRI parameters were used to create receiver operating characteristic (ROC) curves for evaluating the

area under the curve (AUC) and identifying the optimal cut-off value that maximized both sensitivity and specificity. Positive and negative likelihood ratios (PLR and NLR) were also calculated. Statistical analyses were performed using the Statistical Package for the Social Sciences (SPSS) version 22 (IBM, Armonk, NY, USA). Differences were defined as statistically significant at $p < 0.05$. The interobserver reliability for DCE MRI measurement of the tumors was defined by calculating the intraclass correlation coefficients using SPSS version 22. Intraclass correlation coefficients below 0.50, between 0.50 and 0.75, between 0.75 and 0.90, and above 0.90 were defined as poor, moderate, good, and excellent, respectively.

Results

Demographic data of the 47 patients with NPC are presented in Tables 2 and 3. Forty patients (85.1%) were male. The mean age at diagnosis was 45.8 years (range, 17–83 years). Thirty-two patients (68.1%) were positive for pre-treatment plasma EBV DNA, with a median pre-treatment plasma EBV DNA level of approximately 1,296 copies ml^{-1}, and an interquartile range of approximately 12,363. The mean primary tumor size was 459.6 mm^2 (range, 76.3–1261.2 mm^2). The number of patients in the AJCC stage groups I, II, III, and IV were three (6.4%), nine (19.1%), 13 (27.7%), and 22 (46.8%), respectively; in T1, T2, T3, and T4 stages the numbers were 12 (25.5%), six (12.8%), 10 (21.3%), and 19 (40.4%), respectively; whereas in N0, N1, N2, and N3 stages the numbers were seven (14.9%), 25 (53.2%), 10 (21.3%), and five (10.6%), respectively. Only one patient had distant metastasis to the ribs (M1). There was good to excellent interobserver reliability in the measurement of DCE MRI parameters between the two readers with an intraclass correlation coefficients between 0.874 and 0.998 ($p < 0.001$).

Correlation between DCE MRI parameters and plasma EBV DNA levels

The correlations between DCE MRI parameters and plasma EBV DNA levels are summarized in Table 4. Kep_{mean} was significantly negatively correlated with plasma EBV DNA levels (Spearman's rho, –0.328; $p = 0.024$), whereas Ve_{max} was significantly positively correlated with plasma EBV DNA levels (Spearman's rho, 0.341; $p = 0.019$).

Kep_{mean} and Ve_{max} were significantly different between patients with negative and positive plasma EBV DNA ($p = 0.019$ and 0.021, respectively). In addition, Ve_{max} was significantly different between patients with < 2,300 and ≥ 2,300 copies ml^{-1} of plasma EBV DNA ($p = 0.024$) (Fig 1). The ROC curve analysis, cut-off values, sensitivity, specificity, PLR, and NLR values are summarized in Table 5.

Lower Kep_{mean} and higher Ve_{max} were correlated with positive plasma EBV DNA. The optimal cut-off value of Kep_{mean} was 2.1 min^{-1} (AUC, 0.714), whereas that of Ve_{max} was 0.675 (AUC, 0.706) (Figs 1D, 1E, 2D, 2E); however, the latter showed better sensitivity and specificity for determining the plasma EBV DNA status. Ve_{max} higher than the optimal cut-off value of 0.765 (AUC, 0.678) was also correlated with plasma EBV DNA (≥ 2,300 copies ml^{-1}).

Correlation between DCE MRI parameters and NPC stages

Significant correlations were found between DCE MRI parameters and AJCC T stages, N stages, and stage groups (Table 4). Significant correlations between T stages and $Ktrans_{max}$, Kep_{max}, Ve_{mean}, and Ve_{max} were found (Table 4). Of these, the highest correlation coefficient was identified between the T stages and $Ktrans_{max}$ (Spearman's rho, 0.503; $p < 0.001$). $Ktrans_{max}$ was significantly different between the low and high T stages (Fig 3). Higher $Ktrans_{max}$ was

correlated with a higher T stage. The optimal cut-off value of $Ktrans_{max}$ was 1.495 min^{-1} (AUC, 0.767) (Figs 1C, 2C).

N stages were significantly correlated with Vp_{mean} (Spearman's rho, 0.306; $p = 0.037$). Higher Vp_{mean} was correlated with N positive. The optimal cut-off value of Vp_{mean} was 0.125 (AUC, 0.739) (Figs 1F, 2F).

AJCC stage groups were significantly positively correlated with $Ktrans_{max}$ and Ve_{mean} (Spearman's rho, 0.348 and 0.352; $p = 0.017$ and 0.015, respectively); however, only $Ktrans_{max}$ was significantly different between the low and high AJCC stage groups (Fig 3). $Ktrans_{max}$ of more than 1.495 min^{-1} was correlated with the high AJCC stage group (AUC, 0.711).

Discussion

To the best of our knowledge, this is the first study to detect correlations between DCE MRI parameters and plasma EBV DNA status. Both Kep_{mean} and Ve_{max} were significantly correlated with plasma EBV DNA levels (Spearman's rho, –0.328 and 0.341; $p = 0.024$ and 0.019, respectively). Subgroup analysis revealed that lower Kep_{mean} and higher Ve_{max} could fairly accurately differentiate between patients with positive and negative plasma EBV DNA (AUC, 0.714 and 0.706, respectively); however, the accuracy for differentiating patients with plasma EBV DNA ($\geq$ and $< 2{,}300$ copies ml^{-1}) using Ve_{max} was slightly lower (AUC, 0.678).

The underlying mechanism that relates Ve and Kep with plasma EBV status is unclear, but it may be linked to conditions that promote EBV-infected cell growth. Latent EBV infection has a robust correlation with undifferentiated NPC (a subtype of nonkeratinizing carcinoma), which typically includes a massive infiltration of lymphocytes and an inflammatory stroma in histopathology.[3, 5] The inflammatory stroma and abundance of cytokines may increase the

amount of extracellular fluid, reflecting in elevated Ve, as observed in the present study. In addition, the growth of EBV-infected cells may depend on the inflammatory stroma and cytokines.[5] Thus, a low rate constant between the extravascular extracellular space (EES) and blood plasma (Kep) for maintaining inflammatory cells and cytokines may provide the proper conditions for EBV-infected NPC growth.

Significant correlations between T stages and DCE MRI parameters, including $Ktrans_{max}$, Kep_{max}, Ve_{mean}, and Ve_{max}, were detected; of these, the highest correlation coefficient was observed between $Ktrans_{max}$ and T stages. $Ktrans_{max}$ could fairly accurately differentiate high T stages (T3–4) from low T stages (T1–2) (AUC, 0.767). Furthermore, $Ktrans_{max}$ was the only parameter that could fairly accurately differentiate the high (I–II) and the low (III–IV) stage groups (AUC, 0.711). Our results were in accordance with those reported in previous studies. For example, Ni et al[14] studied DCE MRI and diffusion-weighted imaging in patients with NPC and found a positive correlation between NPC clinical stages and Ktrans. Ktrans in NPC stage II was significantly lower than in NPC stages III and IV. Huang et al[15] reported that the initial AUC and Ve were significantly different between low T stages (T1–2) and high T stages (T3–4), likely due to increased neovascularization in the higher T stages and clinical stages of NPC that leads to increased permeability and perfusion within the tumor. High perfusion and permeability of high stage tumors may cause more contrast leakiness (high Ktrans), resulting in more contrast retention in EES (high Ve). High EES (Ve) also promotes the supply of nutrients and oxygenation to high stage tumors.

Patients with NPC and nodal metastasis are more likely associated with a poorer prognosis than those without nodal metastasis. Lymph node morphology examined by conventional MRI alone may not be sufficient for determining metastatic diseases.[16] In these

cases, MRI perfusion can be used as an adjunct tool for better evaluation. Our study revealed a positive correlation between Vp_{mean} of the primary tumor and the N stage (Spearman's rho, 0.306; $p < 0.05$). Higher Vp_{mean} was able to fairly accurately differentiate N positive patients from N negative patients (AUC, 0.739). It is known that the primary tumor has a high intravascular plasma volume or high micro-vessel density that may facilitate cell transfer into the circulatory system and lymph nodes as seen in breast cancer with nodal metastasis.[17] Previous studies showed the effectiveness of DCE MRI for determining nodal metastasis, mostly in breast cancer.[18-20] Information on the association between DCE MRI of primary NPC and the nodal status is still limited and controversial.[21-23] Therefore, more research is needed using larger sample sizes.

The present study found significant correlations between DCE MRI parameters and the plasma EBV DNA status and NPC AJCC stages. A previous study also suggested that integrating pre-treatment plasma EBV DNA into the 8th edition of AJCC staging can improve survival prediction in patients with NPC.[24] Therefore, DCE MRI findings may be another possible biomarker for predicting the clinical outcomes of patients with NPC.

The present study had a few limitations. First, any associations between the area of abnormal perfusion on MRI and the corresponding tumor histopathology were not studied, since NPC is primarily treated with chemoradiation, and entire nasopharyngeal tumor resection is complicated. Second, ROIs were drawn with the axial image, which may not have represented the properties of whole tumors due to tumor heterogeneity. Voxel of interest (VOI) analysis covering the entire tumor may provide more accurate DCE MRI values in a future study. Third, the sample size was small; thus, a prospective study with a larger sample size is considered to be necessary to confirm the reported correlations.

Conclusions

In conclusion, we found that DCE MRI parameters were correlated with the plasma EBV DNA status. A Ve_{max} cut-off value of 0.675 was able to predict patients with positive plasma EBV DNA (sensitivity, 62.5%; specificity, 86.7%), and a Ve_{max} cut-off value of 0.765 could predict patients with plasma EBV DNA ($\geq$ 2,300 copies ml^{-1}; sensitivity 42.1%, specificity 89.3%). DCE MRI parameters were also correlated with NPC AJCC stages, especially the T stages. Therefore, DCE MRI may be useful as an imaging biomarker for patients with NPC.

Funding

This work was supported by the Ratchadaphiseksomphot Endowment Fund [DNS 61_049_30_010_1].

Conflict of interest statement

The authors declare no conflict of interest.

References

1 Bray F, Colombet M, Mery L, et al. Cancer incidence in five continents. Vol. XI (electronic version). Lyon, France: International Agency for Research on Cancer. Available at: http://ci5.iarc.fr. Accessed March 26, 2019.

2 Amin M, Edge S, Greene F, et al. AJCC cancer staging manual .8th ed. New York, USA: Springer, 2017.

3 Tsao SW, Tsang CM, Lo KW. Epstein-Barr virus infection and nasopharyngeal carcinoma. Philos Trans R Soc Lond B Biol Sci 2017;372.

4 Shao JY, Zhang Y, Li YH, et al. Comparison of Epstein-Barr virus DNA level in plasma, peripheral blood cell, and tumor tissue in nasopharyngeal carcinoma. Anticancer Res 2004;24:4059-66.

5 Tsang CM, Tsao SW. The role of Epstein-Barr virus infection in the pathogenesis of nasopharyngeal carcinoma. Virol Sin 2015;30:107-21.

6 Peng H, Chen L, Zhang Y, et al. Survival analysis of patients with advanced-stage nasopharyngeal carcinoma according to the Epstein-Barr virus status. Oncotarget 2016;7:24208-16.

7 Lertbutsayanukul C, Kannarunimit D, Netsawang B, et al. Optimal plasma pretreatment EBV DNA cut-off point for nasopharyngeal cancer patients treated with intensity modulated radiation therapy. Jpn J Clin Oncol 2018;48:467-75.

8 Gaddikeri S, Gaddikeri RS, Tailor T, Anzai Y. Dynamic contrast-enhanced MR imaging in head and neck cancer: techniques and clinical applications. AJNR Am J Neuroradiol 2016;37:588-95.

9 O'Connor JP, Tofts PS, Miles KA, Parkes LM, Thompson G, Jackson A. Dynamic contrast-enhanced imaging techniques: CT and MRI. Br J Radiol 2011;84 Spec No 2:S112-20.

10 Kabadi SJ, Fatterpekar GM, Anzai Y, Mogen J, Hagiwara M, Patel SH. Dynamic contrast-enhanced MR imaging in head and neck cancer. Magn Reson Imaging Clin N Am 2018;26:135-49.

11 Noij DP, de Jong MC, Mulders LG, et al. Contrast-enhanced perfusion magnetic resonance imaging for head and neck squamous cell carcinoma: a systematic review. Oral Oncol 2015;51:124-38.

12 Jittapiromsak N, Hou P, Liu HL, Sun J, Schiffman JS, Chi TL. Dynamic contrast-enhanced MRI of orbital and anterior visual pathway lesions. Magn Reson Imaging 2018;51:44-50.

13 Tofts PS, Brix G, Buckley DL, et al. Estimating kinetic parameters from dynamic contrast-enhanced T1-weighted MRI of a diffusable tracer: standardized quantities and symbols. J Magn Reson Imaging 1999;10:223-32.

14 Ni L, Liu Y. Contrast-enhanced dynamic and diffusion-weighted magnetic resonance imaging at 3.0 T to assess early-stage nasopharyngeal carcinoma. Oncol Lett 2018;15:5294-300.

15 Huang B, Wong CS, Whitcher B, et al. Dynamic contrast-enhanced magnetic resonance imaging for characterising nasopharyngeal carcinoma: comparison of semiquantitative and quantitative parameters and correlation with tumour stage. Eur Radiol 2013;23:1495-502.

16 Fischbein NJ, Noworolski SM, Henry RG, Kaplan MJ, Dillon WP, Nelson SJ. Assessment of metastatic cervical adenopathy using dynamic contrast-enhanced MR imaging. AJNR Am J Neuroradiol 2003;24:301-11.

17 Loiselle CR, Eby PR, Peacock S, Kim JN, Lehman CD. Dynamic contrast-enhanced magnetic resonance imaging and invasive breast cancer: primary lesion kinetics correlated with axillary lymph node extracapsular extension. J Magn Reson Imaging 2011;33:96-101.

18 Bahri S, Chen JH, Yu HJ, Kuzucan A, Nalcioglu O, Su MY. Can dynamic contrast-enhanced MRI (DCE-MRI) predict tumor recurrence and lymph node status in patients with breast cancer? Ann Oncol 2008;19:822-4.

19 Liu C, Ding J, Spuhler K, et al. Preoperative prediction of sentinel lymph node metastasis in breast cancer by radiomic signatures from dynamic contrast-enhanced MRI. J Magn Reson Imaging 2019;49:131-40.

20 Chen Y, Li R, Chen T, et al. Whole-tumour histogram analysis of pharmacokinetic parameters from dynamic contrast-enhanced MRI in resectable oesophageal squamous cell carcinoma can predict T-stage and regional lymph node metastasis. Eur J Radiol 2019;112:112-20.

21 Huang B, Kwong DL, Lai V, Chan Q, Whitcher B, Khong PL. Dynamic contrast-enhanced magnetic resonance imaging of regional nodal metastasis in nasopharyngeal carcinoma: correlation with nodal staging. Contrast Media Mol Imaging 2017;2017:4519653.

22 Zheng D, Chen Y, Chen Y, et al. Dynamic contrast-enhanced MRI of nasopharyngeal carcinoma: a preliminary study of the correlations between quantitative parameters and clinical stage. J Magn Reson Imaging 2014;39:940-8.

23 Lai V, Li X, Lee VH, et al. Nasopharyngeal carcinoma: comparison of diffusion and perfusion characteristics between different tumour stages using intravoxel incoherent motion MR imaging. Eur Radiol 2014;24:176-83.

24 Kitpanit S, Jittapiromsak N, Sriyook A, et al. Comparison between the seventh and eighth edition of the AJCC/UICC staging system for nasopharyngeal cancer integrated with pretreatment plasma Epstein-Barr virus DNA level in a non-Chinese population: secondary analysis from a prospective randomized trial. Jpn J Clin Oncol 2019. [Epub ahead of print].

Tables

Table 1

Definitions and units of dynamic contrast enhanced (DCE) magnetic resonance imaging (MRI) parameters according to the extended Tofts model.

Parameters	Definitions	Unit
Ktrans	Rate constant for the transfer of the contrast agent from the plasma to the extravascular extracellular space (EES)	min^{-1}
Kep	Rate constant for the transfer of the contrast agent from the EES to the plasma	min^{-1}
Ve	Volume of EES per unit volume of tissue (fractional volume of EES)	None
Vp	Plasma volume (fractional volume of vascular plasma space)	None

Table 2

Patient demographics and plasma Epstein-Barr virus (EBV) DNA levels.

Data parameters	Number of patients (n = 47)
Sex	
Male (%)	40 (85.1%)
Female (%)	7 (14.9%)
Mean age in years ± standard deviation (range)	45.8 ± 2.1 (17–83)
Tumor pathology	
Squamous cell carcinoma, nonkeratinizing (%)	45 (95.7%)
Differentiated (WHO IIA)	4 (8.5%)
Undifferentiated (WHO IIB)	41 (87.2%)
Carcinoma, not otherwise specified (%)	2 (4.3%)
Mean size of the primary tumor in mm^2 ± standard deviation (range)	459.6 ± 298.5 (76.3-1261.2)
Pre-treatment plasma median EBV DNA copies ml^{-1} (interquartile range)	1,296 (0–12,363)
Pre-treatment plasma EBV DNA	
Negative (%)	15 (31.9%)
Positive (%)	32 (68.1%)
Pre-treatment plasma EBV DNA level	
< 2,300 copies ml^{-1} (%)	28 (59.6%)
≥ 2,300 copies ml^{-1} (%)	19 (40.4%)

WHO, World Health Organization

Table 3

Staging according to the eighth edition of the American Joint Committee on Cancer (AJCC) staging criteria.

Data parameters	Number of patients (n = 47)
T stage	
Low (%)	18 (38.3%)
T1 (%)	12 (25.5%)
T2 (%)	6 (12.8%)
High (%)	29 (61.7%)
T3 (%)	10 (21.3%)
T4 (%)	19 (40.4%)
N stage	
N negative/N0 (%)	7 (14.9%)
N positive (%)	40 (85.1%)
N1 (%)	25 (53.2%)
N2 (%)	10 (21.3%)
N3 (%)	5 (10.6%)
M stage	
M0 (%)	46 (97.9%)
M1 (%)	1 (2.1%)
AJCC stage group	
Low-stage group (%)	12 (25.5%)
I (%)	3 (6.4%)
II (%)	9 (19.1%)
High-stage group (%)	35 (74.5%)
III (%)	13 (27.7%)
IV (%)	22 (46.8%)

Table 4

Correlation between dynamic contrast enhanced (DCE) magnetic resonance imaging (MRI) parameters and Epstein-Barr virus (EBV) DNA levels, as well as the American Joint Committee on Cancer (AJCC) T stages, N stages, and stage groups.

DCE MRI parameters		Spearman's rho correlation coefficients							
		Plasma EBV DNA	*p* value	T stage	*p* value	N stage	*p* value	Stage group	*p* value
Ktrans	Mean	-0.232	0.117	0.282	0.054	-0.071	0.637	0.136	0.361
	Max	-0.105	0.480	0.503*	0.000	0.050	0.739	0.348*	0.017
Kep	Mean	-0.328*	0.024	0.085	0.571	-0.056	0.708	-0.032	0.831
	Max	-0.207	0.162	0.376*	0.009	0.006	0.966	0.284	0.053
Ve	Mean	0.062	0.678	0.447*	0.002	0.043	0.775	0.352*	0.015
	Max	0.341*	0.019	0.294*	0.045	0.221	0.136	0.238	0.106
Vp	Mean	0.206	0.166	0.122	0.415	0.306*	0.037	0.240	0.105
	Max	0.235	0.111	0.124	0.405	0.287	0.050	0.255	0.084

*Significant at $p < 0.05$

Table 5

Comparison of significant dynamic contrast enhanced (DCE) magnetic resonance imaging (MRI) parameters with optimal cut-off values between negative and positive plasma Epstein-Barr virus (EBV) DNA, plasma EBV DNA (< and ≥ 2,300 copies ml^{-1}), low and high T stages, N negative and positive, and low and high stage groups.

Groups	DCE MRI parameters	AUC of ROC curve (95% CI)	Cut-off value	Sensitivity	Specificity	PLR	NLR	*p* value
Negative vs. positive plasma EBV DNA	Kep_{mean}	0.714 (0.565–0.862)	2.1	53.3%	75%	2.1	0.6	0.019*
	Ve_{max}	0.706 (0.555–0.857)	0.675	62.5%	86.7%	4.7	0.4	0.021**
Plasma EBV DNA < vs. ≥ 2,300 copies ml^{-1}	Ve_{max}	0.678 (0.514–0.841)	0.765	42.1%	89.3%	3.9	0.6	0.024**
Low vs. high T stages	$Ktrans_{max}$	0.767 (0.63–0.904)	1.495	65.5%	88.9%	5.9	0.4	0.002**
N negative vs. positive	Vp_{mean}	0.739 (0.573–0.906)	0.125	50%	85.7%	3.5	0.6	0.045**
Low vs. high stage groups	$Ktrans_{max}$	0.711 (0.546–0.875)	1.495	54.3%	83.3%	3.3	0.5	0.035**

ROC, receiver operating characteristic AUC, area under the curve; CI, confidence interval; PLR, positive likelihood ratio; NLR, negative likelihood ratio.
**p* values calculated using Mann-Whitney U tests; ***p* values calculated using unpaired t-tests.

Figures

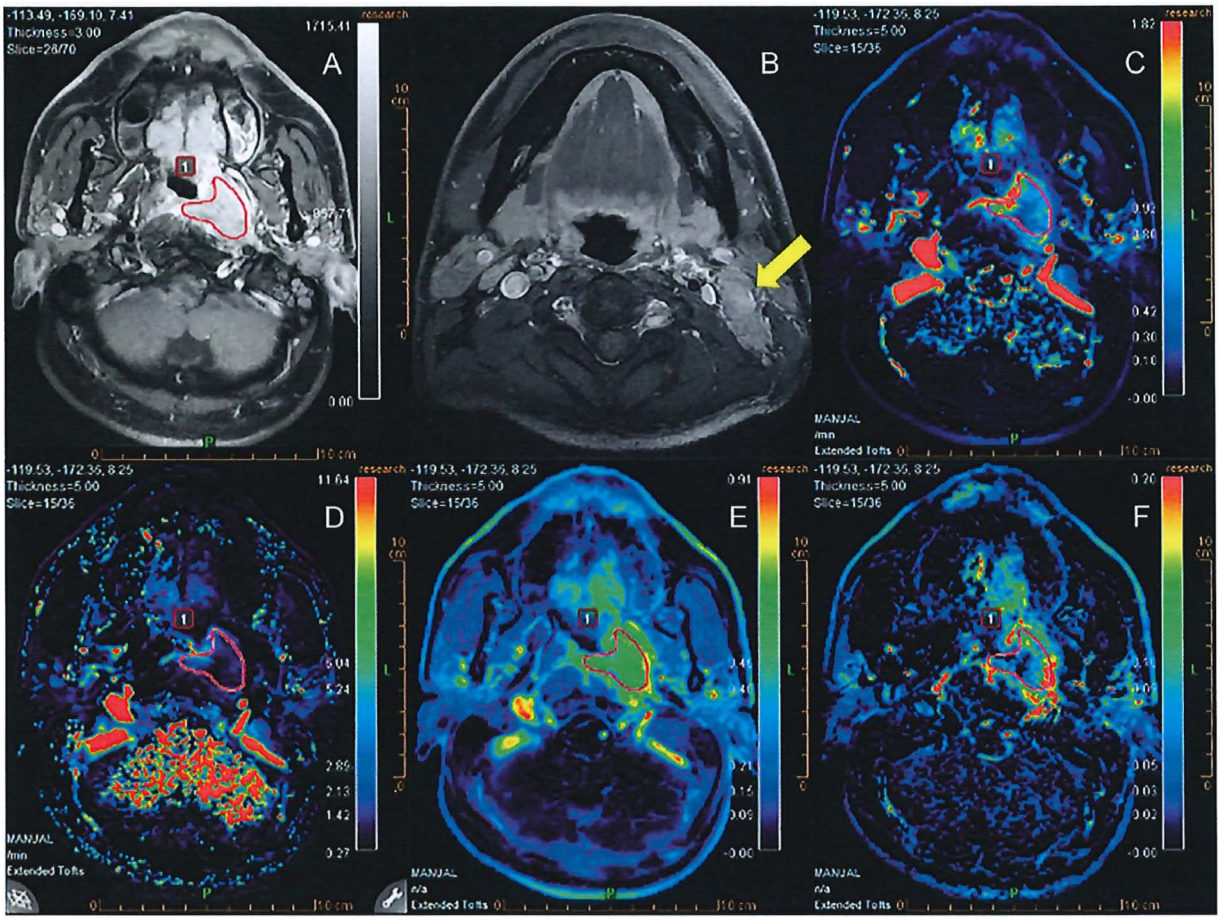

Figure 1 A 47-year-old male with nasopharyngeal carcinoma (NPC) stage group IV (T4N1M0; based on the American Joint Committee on Cancer staging criteria) and a pre-treatment plasma Epstein-Barr virus (EBV) DNA level of 2,580 copies ml^{-1}. (A) An axial contrast-enhanced T1-weighted image showing an enhanced tumor predominantly involved with the left-sided nasopharynx, left parapharyngeal space, and left pre-vertebral muscle (region of interest shown in red) with intracranial extension to the left cavernous sinus (not shown). (B) Axial contrast-enhanced T1-weighted image shows an enhanced matted left level II lymph node (arrow). (C) Ktrans, (D) Kep, (E) Ve, and (F) Vp maps with $Ktrans_{max}$, 1.82 min^{-1}; Kep_{mean}, 1.34 min^{-1}; Ve_{max},

0.84; and Vp_{mean}, 0.08.

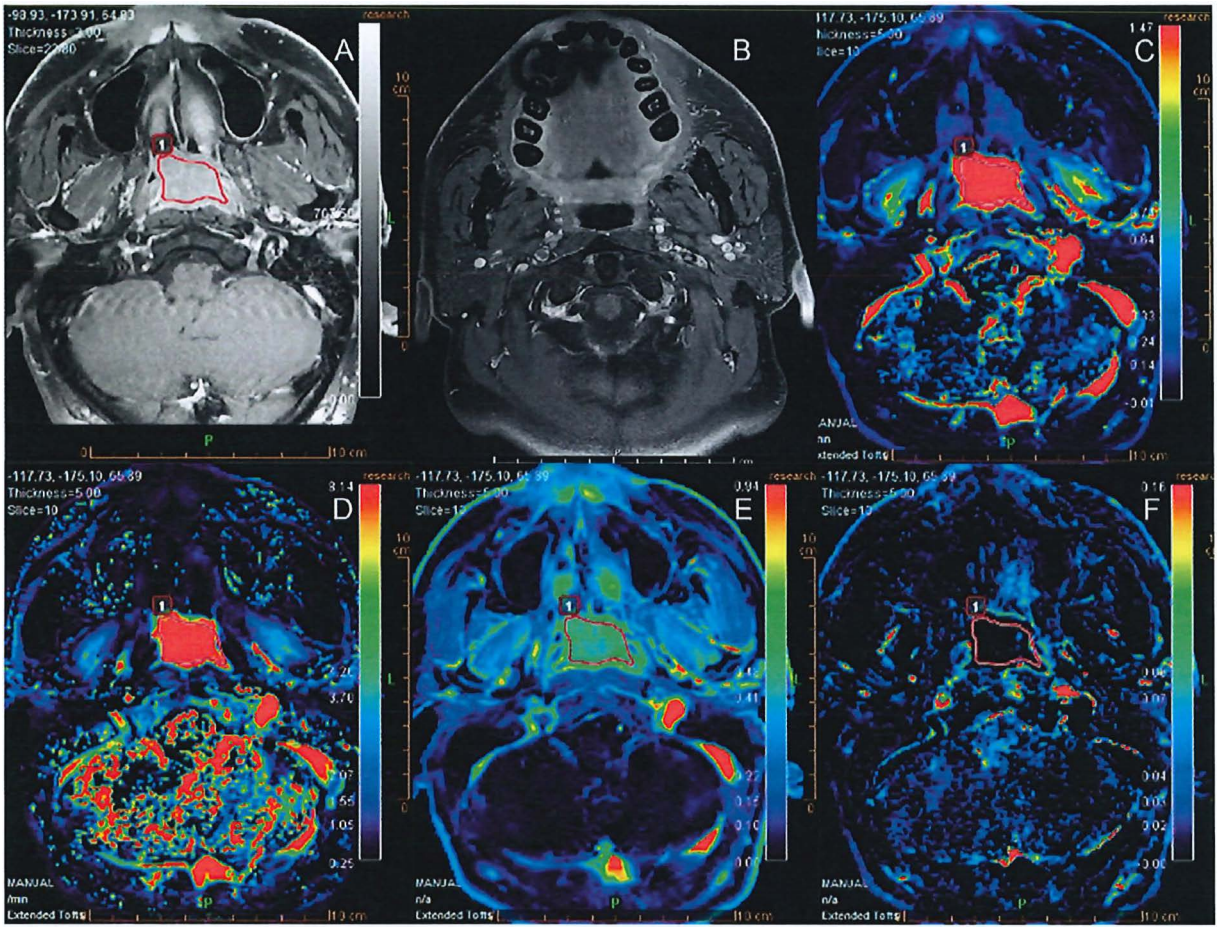

Figure 2 A 45-year-old male with nasopharyngeal carcinoma (NPC) stage group I (T1N0M0; based on the American Joint Committee on Cancer staging criteria) and a pre-treatment plasma Epstein-Barr virus (EBV) DNA level of < 316 copies ml^{-1}. (A) Axial contrast-enhanced T1-weighted image shows an enhanced tumor involving both sides of the nasopharynx (region of interest shown in red). (B) Axial contrast-enhanced T1-weighted image shows no metastatic lymph node. (C) Ktrans, (D) Kep, (E) Ve, and (F) Vp maps with $Ktrans_{max}$, 1.47 min^{-1}; Kep_{mean}, 7.29 min^{-1}; Ve_{max}, 0.64; and Vp_{mean}, 0.01.

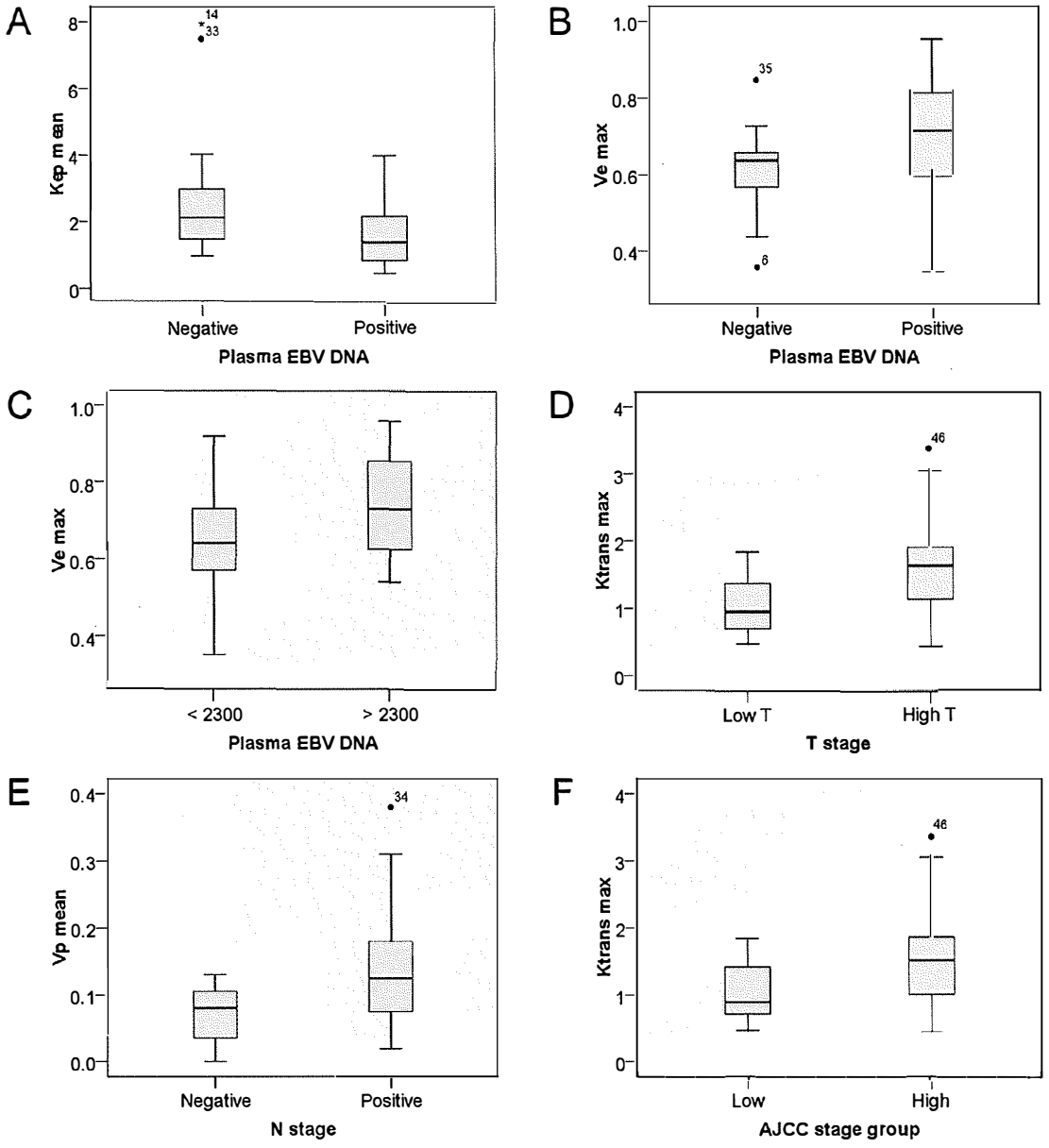

Figure 3 Box plots showing significantly different dynamic contrast enhanced (DCE) magnetic resonance imaging (MRI) parameters in subgroup analysis ($p < 0.05$). (A) Kep_{mean} and (B) Ve_{max} of plasma Epstein-Barr virus (EBV) DNA negative and positive, (C) Ve_{max} of plasma EBV DNA (< and ≥ 2,300 copies ml^{-1}), (D) $Ktrans_{max}$ of low and high T stages, (E) Vp_{mean} of N negative and N positive, and (F) $Ktrans_{max}$ of low and high American Joint Committee on Cancer stages.

ลงชื่อ .....ผู้รับทุน

(แพทย์หญิงณัชวาล จิตตภิรมย์ศักดิ์)

ลงชื่อ.....อาจารย์อาวุโส

(รองศาสตราจารย์ นายแพทย์ชวลิต เลิศบุษยานุกูล)